Acta of Bioengineering and Biomechanics
Vol. 17, No. 2, 2015

Original paper
DOI: 10.5277/ABB-00142-2014-03

Corneal hyper-viscoelastic model: derivations, experiments, and simulations

PENG SU, YANG YANG*, JINGJING XIAO, YANMING SONG

School of Mechanical Engineering and Automation, BeiHang University, People's Republic of China.

Purpose: The aim of this study is to propose a method to construct corneal biomechanical model which is the foundation for simulation of corneal microsurgery. Methods: Corneal material has two significant characteristics: hyperelastic and viscoelastic. Firstly, Mooney–Rivlin hyperelastic model of cornea obtained based on stored-energy function can be simplified as a linear equation with two unknown parameters. Then, modified Maxwell viscoelastic model of the cornea, whose analytical form is consistent with the generalized Prony-series model, is proposed from the perspective of material mechanics. Results: Parameters of the model are determined by the uniaxial tensile tests and the stress-relaxation tests. Corneal material properties are simulated to verify the hyper-viscoelastic model and measure the effectiveness of the model in the finite element simulation. On this basis, an *in vivo* model of the corneal is built. And the simulation of extrusion in vivo cornea shows that the force is roughly nonlinearly increasing with displacement, and it is consistent with the results obtained by extrusion experiment of in vivo cornea. Conlusions: This paper derives a corneal hyper-viscoelastic model to describe the material properties more accurately, and explains the mathematical method for determination of the model parameters. The model is an effective biomechanical model, which can be directly used for simulation of trephine and suture in keratoplasty. Although the corneal hyper-viscoelastic model is taken as the object of study, the method has certain adaptability in biomechanical research of ophthalmology.

Key words: *cornea, biomechanics, constitutive model, hyperelastic, viscoelastic*

1. Introduction

Biomechanical properties of the cornea have important reference value for diagnosis and treatment of corneal diseases, maintaining corneal shape, the research of artificial cornea, etc. The biomechanical model is the foundation for numerical simulation of corneal microsurgery using a variety of techniques, such as finite element technique, engineering, and mathematics [4], and the simulation can become a valuable tool to plan ophthalmosurgical procedures [12].

Biomechanical modeling of soft tissue is one of the applications of the deformation model. Usually the functional relationship between the stress tensor and the strain tensor is called constitutive model, a mathematical model to reflect the macroscopic properties of the material. In the early 1970s, Wildnauer et al. [28] tested stress-strain relationships and failure strength of the human skin in different humidity by the uniaxial tensile test, an in vitro measurement method. Besides, *in vivo* measurement is possible with the development of science and technology. Hendriks et al. [15] measured mechanical behavior of epidermis and dermis *in vivo* skin, and built constitutive models of different skin layers.

As a typical representative of soft biological tissue, the constitutive model of the cornea has been derived in many studies. In order to study the behaviour of the cornea under different loading states and provide improved predictions of the mechanical response to disease and injury, nonlinear finite-element modelling has been used in conjunction with experiments [1]. Studer et al. [26] proposed a biomechanical

* Corresponding author: Yang Yang, School of Mechanical Engineering and Automation, Beihang University, XueYuan Road No. 37, HaiDian District, Beijing 100191, China. Tel: +86 01082338386, e-mail: yang_mech@126.com

Received: July 27th, 2014
Accepted for publication: August 28th, 2014

model of human cornea based on stromal microstructure, where the constitutive mechanical law includes collagen fiber distribution based on X-ray scattering analysis, collagen cross-linking, and fiber uncrimping. On this basis, they reproduced inflation and extension experimental data in simulation. Pandolfi et al. [23] employed a fiber-matrix constitutive model and proposed a numerical model for human cornea, which is able to account for its mechanical behavior in healthy conditions or in the presence of keratoconus under increasing values of the intraocular pressure. Assuming that the cornea can be approximated as a homogenous spherical structure with a constant thickness, Anderson et al. [1] developed material constitutive relationship based on mathematical analysis of corneal inflation tests, and constructed finite-element models that are able to trace the performance of cornea upon exposure to disease, injury or elevated intra-ocular pressure. Similarly, on the basis of swelling mechanics, Karalis et al. [19] presented a theoretical model for corneal swelling with respect to aqueous inflow, based on corneal dimensions and mechanical and chemical properties, which can explain how glaucoma or hypotony come about. In order to simulate the procedure of intrastromal photorefractive keratectomy, Hameed-Sayed et al. [12] provided a three-dimensional model of the cornea with typical parameters. Besides, the finite element method with web-spline computer modeling was applied to study the increase of corneal surface temperature during microwave irradiation [20].

There are two significant characteristics of corneal material: hyperelastic and viscoelastic. Hyperelastic theory, established by Mooney and Rivlin, may describe the main features of biological soft tissues, including deformation, non-compressibility, and continuous deformation recovery at a specified time [7], [22]. Furthermore, biological tissue is composed of solid matter and liquid matter. And in biomechanics and biorheology, one of the fundamental theories that may better reflect the interaction between solid and liquid in the biological tissue is viscoelastic theory [25]. The hyper-viscoelastic properties of the cornea are described by some mechanical behaviours such as short-term stress–strain and stress-relaxation. And many scholars tested human corneas and porcine corneas to determine the behaviours under inflation tests or uniaxial tests [9], [30]. Besides, Woo and Bryant measured material constants of the cornea according to nonlinear stress-strain relationship obtained by swelling tests [5], [29]. In the previous studies, there are some differences in the accurate results under different testing conditions or experimental specifications [18], [21], [26], [30].

For a more accurate description of corneal material properties, this paper derives biomechanical model of the cornea based on hyper-viscoelastic theory, which is a relatively simple mathematical model. The parameters of the model are determined by uniaxial-tensile tests and stress-relaxation tests, and its availability can be verified by experiment and simulation of extrusion *in vivo* cornea. The derived model that is the foundation for simulation of corneal microsurgery can be used to improve the understanding of the biomechanical behaviour of the cornea.

2. Materials and methods

2.1. Biological structures and biomechanical properties

The cornea has the macroscopic structure of a thin shell in front wall of the eye, as seen in Fig. 1. Corneal central zone (i.e., pupillary zone) is approximately spherical where radius of curvature at each point is roughly equal, whereas the pericentral zone and the peripheral zone are relatively flat. Assuming corneal surface is substantially spherical, it has a different thickness at each position, and pupillary zone is the thinnest. Geometric parameters of human cornea are shown in Table 1.

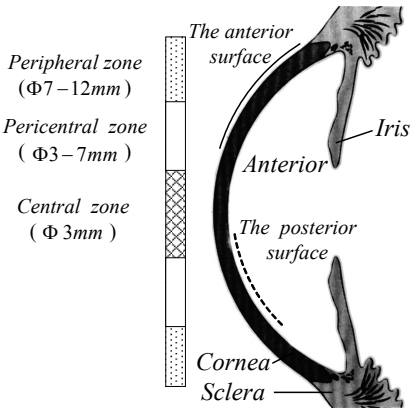

Fig. 1. Schematic of corneal structure

Table 1. Corneal geometric parameters [mm]

Parameter	Value	Parameter	Value
Axial length	26.50	Horizontal diameter	11.20
Corneal mean thickness	0.67	vertical diameter	11.00
Central thickness	0.55	Pericentral thickness	0.72
Peripheral thickness	1.00	Corneal anterior radius	7.80
Corneal posterior radius	6.80		

Histologically, cornea can be divided into five layers by studying its structures and properties using confocal microscopy, including epithelium (the thickness is about 35–55 micrometer), lamina elastica anterior (about 12 micrometer), stroma (about 500 micrometer), lamina elastica posterior (about 10–12 micrometer), and endothelium (about 5 micrometer) [1], [8], [10]. The biomechanical properties of the cornea are primarily derived from the stroma [14]. Stroma is the main load-bearing part, accounting for about 90% of corneal thickness. The front part of the stroma assumes a greater role in biomechanics due to more dense lamellar arrangement than the rear part, and this characteristic makes cornea lighter and more flexible [11]. Many researchers have studied the cornea as a whole, but they did not point out its structural layer corresponding to the measured parameters. We can consider approximately that most results are biomechanical responses of stroma, according to corneal morphology and biomechanical properties [14], [26], [27].

From macro perspective, the cornea has a variety of features, such as diversity, anisotropic, nonlinear, and viscoelastic [24]. Normally cornea is in a tensioned state, and it is difficult to quantitatively describe the corneal biomechanical properties, as there are many factors that can affect them, e.g., age [26], gender, IOP (i.e., Intra-ocular pressure) [19], and ocular temperature [20], etc.

Notably, the biological tissue normally presents the internal stress in the normal physiological state. Corneal internal stress is generated because the difference between IOP and atmospheric pressure is approximately 17.5 mmHg (11–21 mmHg). When the tissue is removed from the organism, it will shrink due to loss of the stress. Besides, corneal constraints should be considered due to cornea is not isolated in the eyeball. Anderson et al. [1] used 40° hinged support to fix the cornea border, joining the torsion spring in the hinged support to more accurately express scleral fixation [1]. However, they did not take into account the full contact between cornea and sclera that affected the simulation results. Referencing Fig. 1, there is a close association between cornea and sclera, and they compose the outer wall of the eye. Also, the sclera also is both anisotropic and viscoelastic [2], [3].

2.2. Hyperelastic modeling

A study objective of the hyperelasticity is to establish the stored-energy function associated with the deformation parameter, and give a mechanical explanation. There are many ways to establish the stored-energy function. Theoretically, this can be explained based on thermodynamic theory, statistical theory, and internal molecular mechanism [22].

A characteristic of hyperelastic material is that there is a potential stored-energy function W. For most of hyperelastic material, $W = W(C) = W(I_1, I_2, I_3)$, which is the potential energy of the second Piola–Kirchhoff stress tensor S described as

$$S = \frac{\partial W}{\partial E} = 2\frac{\partial W(I_1, I_2, I_3)}{\partial C}, \tag{1}$$

where E is a component of Green–Lagrangian strain tensor, and C is the right Cauchy–Green deformation tensor. I_1, I_2, and I_3 are three basic invariants of tensor C.

Assuming λ_i (i = 1, 2, 3) represents main extension ratio, principal strain ε_i can be obtained by $\varepsilon_i = \lambda_i - 1$. The relationships between the basic invariants of tensor C and the main extension ratio λ_i can be expressed as

$$\begin{gathered} I_1 = \lambda_1^2 + \lambda_2^2 + \lambda_3^2, \\ I_2 = \lambda_1^2\lambda_2^2 + \lambda_2^2\lambda_3^2 + \lambda_3^2\lambda_1^2, \quad I_3 = \lambda_1^2\lambda_2^2\lambda_3^2. \end{gathered} \tag{2}$$

According to equation (1), the energy function of the material is determined from

$$S = 2\left(\frac{\partial W}{\partial I_1}\frac{\partial I_1}{\partial C} + \frac{\partial W}{\partial I_2}\frac{\partial I_2}{\partial C} + \frac{\partial W}{\partial I_3}\frac{\partial I_3}{\partial C}\right). \tag{3}$$

For the hyperelastic material, stored-energy W can be decomposed into isochoric part $\overline{W}$ and hydrostatic part W_h in the following form [7]

$$W = \overline{W} + W_h = f(\bar{I}_1 - 3, \bar{I}_2 - 3) + p(J-1), \tag{4}$$

where $\bar{I}_1 = J^{-\frac{2}{3}} I_1$ and $\bar{I}_2 = J^{-\frac{4}{3}} I_2$ represent the first and second invariant of isochoric tensor $\overline{C}$. $J = I^{\frac{1}{2}}$ represents volume ratio of deformation, i.e., the expansion ratio. p is hydrostatic pressure, which can be expressed as

$$p(J-1) = \sum_{i=1}^{N} \frac{1}{D_i}(J-1)^2. \tag{5}$$

Then, strain stored-energy function, which has complete multinomial form, can be described as

$$W = \sum_{i,j=0}^{N} C_{ij}(\bar{I}_1 - 3)^i(\bar{I}_2 - 3)^j + \sum_{i=1}^{N} \frac{1}{D_i}(J-1)^2, \tag{6}$$

where N is the order of the expression; model coefficient C_{ij} reflects the characteristics of the material; bulk modulus D_i indicates the compressibility of the material.

The above equation is Mooney–Rivlin hyperelastic model of cornea [22]. For corneal material which can be assumed to be an incompressible material [18], [30], there is $I_3 = \lambda_1^2\lambda_2^2\lambda_3^2 = 1$. In this case,

$$\bar{I}_1 = I_1, \quad \bar{I}_2 = I_2, \quad \lambda_3 = \frac{1}{\lambda_1\lambda_2}, \quad J = 1. \tag{7}$$

The coefficients of stored-energy function W can be determined according to the experimental images. Based on the stored-energy function that has two coefficients, the experimental data are fitted according to the analysis of corneal stress-strain curve [5], [9], [30]. So the formula (6) can be expressed as

$$W = C_{10}(\bar{I}_1 - 3) + C_{01}(\bar{I}_2 - 3). \tag{8}$$

According to equation (2), the relationship between the principal stress t_i and the main extension ratio λ_i can be expressed as [17]

$$t_i = 2\lambda_i\left[\frac{\partial W}{\partial I_1} + (\lambda_{i^-}^2 + \lambda_{i^+}^2)\frac{\partial W}{\partial I_2} + \lambda_{i^-}^2\lambda_{i^+}^2\frac{\partial W}{\partial I_3}\right], \tag{9}$$

where i, i^-, and i^+ are different values that belong to interval (1, 2, 3).

By equation (2) and equation (8), the first two basic invariants of tensor C can be obtained as

$$I_1 = \lambda_1^2 + \lambda_2^2 + \frac{1}{\lambda_1^2\lambda_2^2}, \quad I_2 = \lambda_1^2\lambda_2^2 + \frac{1}{\lambda_1^2} + \frac{1}{\lambda_2^2}. \tag{10}$$

According to equation (3), equation (9) can be rendered in the form

$$t_i = \frac{2}{\lambda_i}\left(\lambda_i^2 - \frac{1}{\lambda_1^2\lambda_2^2}\right)\left(\frac{\partial W}{\partial I_1} + \lambda_{i^-}^2\frac{\partial W}{\partial I_2}\right), \tag{11}$$

where i and i^- are different values that belong to interval (1, 2).

For the incompressible material, hydrostatic pressure does not affect the strain state. So, a hydrostatic pressure p can be superimposed on equation (11), i.e., principal stress can be expressed as $t_1 + p$, $t_2 + p$, and p. In uniaxial tensile test, $t_2 = 0$. In this case,

$$\lambda_1 = \lambda = l/l_0, \quad \lambda_2^2 = \lambda_3^2 = \lambda^{-1}, \tag{12}$$

where l_0 is the initial length, and l is the tensile displacement. So, equation (2) can be expressed as

$$I_1 = \lambda^2 + \frac{2}{\lambda}, \quad I_2 = 2\lambda + \frac{1}{\lambda^2}, \quad I_3 = 1. \tag{13}$$

According to equation (11) and equation (12), principal stress t_1 becomes

$$t_1 = 2\left(\lambda - \frac{1}{\lambda^2}\right)\left(\frac{\partial W}{\partial I_1} + \frac{1}{\lambda}\frac{\partial W}{\partial I_2}\right). \tag{14}$$

Therefore, hyperelastic model of cornea can be simplified as a linear equation of two unknowns, i.e.,

$$Y = C_{10} + C_{01}X, \tag{15}$$

where $X = \frac{1}{\lambda}$ and $Y = \frac{t_1}{2\left(\lambda - \frac{1}{\lambda^2}\right)}$.

According to the measured stress value under different draw ratio, a straight line is fitted to obtain C_{10} and C_{01}.

2.3. Viscoelastic modeling

Although there are some differences in material behaviors between elastic and viscoelastic, such as timeliness, deformation properties and material breakages, both of them are able to describe anti-deformation and deformation recovery of the material. Many kinds of viscoelastic models can be composed of discrete elastic elements and viscous elements [6]. Maxwell model ([M]) and Kelvin model ([K]) are the basic models of viscoelasticity [25]. [M] is a series connection of a spring and a damper, whereas [K] consists of a spring and a damper connected in parallel. On the basis of the basic models, other models can be considered as combinations of elastic and viscous elements, such as generalized Maxwell model, Burgers model, etc.

The existence of corneal viscoelastic behavior had been verified by many experimental results [2], [13]. Referring to generalized Maxwell model, the viscoelastic constitutive model of the cornea is established, which consists of [M] model in parallel. Because there is a series damper in each [M], the internal stress of material would become near to zero if the time of external load is longer enough. Therefore, in order to describe the material properties more accurately, an elastic element is connected in parallel with the generalized Maxwell model, as shown in Fig. 2. We define the model as modified Maxwell viscoelastic model of the cornea. The solid property, shown by the paralleled elastic element [E], reflects the residual stress of cornea in the relaxation curves.

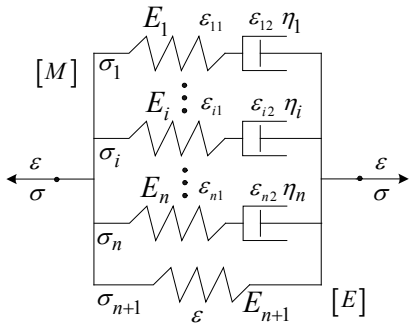

Fig. 2. The modified Maxwell viscoelastic model of the cornea

The stress σ and strain ε of viscoelastic model (as shown in Fig. 2) can be described in the following form

$$\sigma = \sum_{i=1}^{n+1} \sigma_i, \quad \varepsilon = \varepsilon_{i1} + \varepsilon_{i2} \quad (i = 1, 2, ..., i, ..., n), \tag{16}$$

where σ_i is the stress in the i-th sub-model; ε_{i1} is the strain of the i-th elastic element; ε_{i2} is the strain of the i-th viscous element.

According to equation (16), the constitutive equation of [M] model can be rendered in the form

$$\sum_{i=1}^{n} \sigma_i + \sum_{i=1}^{n} \frac{\eta_i}{E_i} \sigma_i = \sum_{i=1}^{n} \eta_i \varepsilon_i . \tag{17}$$

Using Laplace transform, the constitutive equation in transformed space is given by

$$\overline{\sigma} = \sum_{i=1}^{n} \left[\frac{\eta_i s}{1 + (\eta_i / E_i) s} \right] \overline{\varepsilon} = \sum_{i=1}^{n} \left[\frac{\eta_i s}{1 + \tau_i s} \right] \overline{\varepsilon}, \tag{18}$$

where $\tau_i = \eta_i / E_i$. At the fixed temperature, the differential equation is solved by Unit Step Function $\varepsilon = H(t)$, and stress response (i.e., relaxation function) is expressed by

$$E(t) = \sum_{i=1}^{n} E_i e^{-t/\tau_i}, \tag{19}$$

where τ_i is relaxation time of the i-th [M] model.

Therefore, corneal viscoelastic model, shown in Fig. 2, can be defined as

$$E(t) = \sum_{i=1}^{n} E_i e^{-t/\tau_i} + E_{n+1}. \tag{20}$$

The analytical form of the above equation is consistent with the generalized Prony-series model where E_i and τ_i are the model parameters; n is the number of Prony-series; E_{n+1} is the static elastic modulus (i.e., the long-term relaxation modulus), and

$$E_{n+1} = \frac{\sigma_\infty}{\varepsilon_0}, \tag{21}$$

where σ_∞ is residual stress and ε_0 is constant strain.

The model can accurately describe material viscoelastic, and its parameters are also relatively easy to be obtained by numerical fitting based on stress-relaxation tests.

Assuming the load is F_i, strain is ε_i, cross-sectional area of specimen is A in each test, and the test number is k, instantaneous elastic modulus is given by

$$E_i = \frac{1}{kA} \sum_{i=1}^{k} \frac{F_i}{\varepsilon_i}. \tag{22}$$

Assuming the initial load as F_0 and the initial elastic modulus as E_0, the constant strain is determined from

$$\varepsilon_0 = \frac{F_0}{AE_0}. \tag{23}$$

Based on the experimentally measured tensile force $F(t)$, relaxation modulus $E(t)$ is obtained from

$$E(t) = \frac{F(t)}{A\varepsilon} = \frac{\sigma(t)}{\varepsilon}. \tag{24}$$

According to master curve of the relaxation modulus, the relaxation function $E(t)$ can be fitted by Prony-series.

For fitting of the Prony-series, defining a sequence of positive numbers as $[\tau_i](i = 1, 2, ..., i, ..., n)$, which is uniformly distributed on the logarithmic coordinate axis, the data fitting problem is to determine the undetermined coefficients of the Prony-series E_i ($E_i > 0$). Besides, the coefficients can make the minimum difference between function value of Prony-series $E(t)$ and relaxation modulus $E(t_n)$ in the test time t_n, i.e.,

$$\min E(t) - E_\infty = \sum_{i=1}^{n} E_i e^{-t/\tau_i} \quad (i = 1, 2, ..., i, ..., n). \tag{25}$$

Define $\{A\} = E(t) - E_\infty$, $\{B\} = e^{-t/\tau_i}$, and $\{C\} = E_i$, then the formula above can be transformed into a linear programming problem

$$\min \text{size} \left| \sum_{i=1}^{n} \{B\}\{C\} - \{A\} \right|. \tag{26}$$

The hyperelastic model and viscoelastic model of the cornea are established respectively. The hyperelastic property of deformation-recovery and time-dependent viscoelastic property should be considered at the same time under loading conditions. In general, it can be attributed to the non-linear hyper-viscoelastic

problem. It is a complex problem in the field of solid mechanics, because the relationship between the deformation rate and time rate is a series of energy conversion behavior. In this paper, two properties add up to affect the state of corneal tissue, but not to consider the relationship which will be discussed as the following research contents.

3. Results

3.1. The parameters of the corneal model

In order to get accurate data under our testing condition that is consistent with the later extrusion experimentation, the parameters of the corneal model are obtained by uniaxial tensile test and stress-relaxation test, and methods of these tests are the same as previous study [9], [30]. In this paper, porcine corneas are taken as the test subjects because it is easier to obtain than human cornea, and test subjects are 20 fresh porcine eyes, slaughtered within eight hours. Corneas are cut into rectangular strips that are about 12 mm × 4 mm, as shown in Fig. 3(a) and (b).

Corneal strips should be placed for two hours in order to eliminate the effects of internal stress, and the strips of naturally curved cornea are straightened to conduct the test. During the test, scleral strips and corneal edges are clamped with biological material holder, as shown in Fig. 3(c).

In the uniaxial tensile tests, the strips are stretched until they broke in the speed of 20 mm/min. Ten times tests would be done respectively, and the related data are recorded, such as axial tension F and strip length l. Then, the stress and the strain can be calculated by $\sigma = F/A$ and $\varepsilon = l/l_0 - 1$. In the formula, A is the initial value of cross-sectional area where the thickness is corneal mean thickness, and l_0 is the initial length. The relationship of stress-strain is indicated in Fig. 4(a) based on Gauss curve fitting about the average values of test datas, and the fitting equation is expressed by

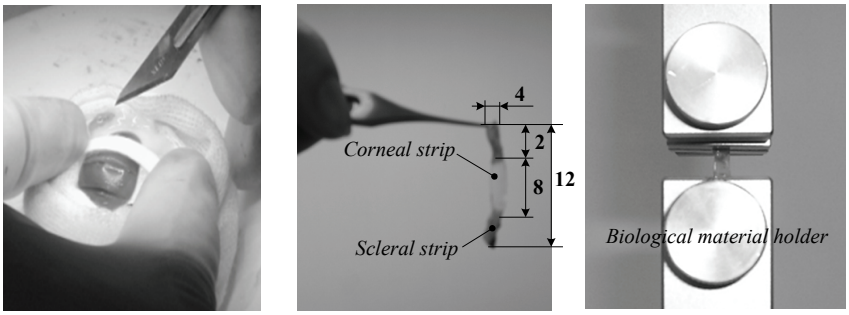

(a) (b) (c)

Fig. 3. Corneal uniaxial tensile test: (a) cornea is cut into rectangular strips, (b) corneal strip, (c) the test

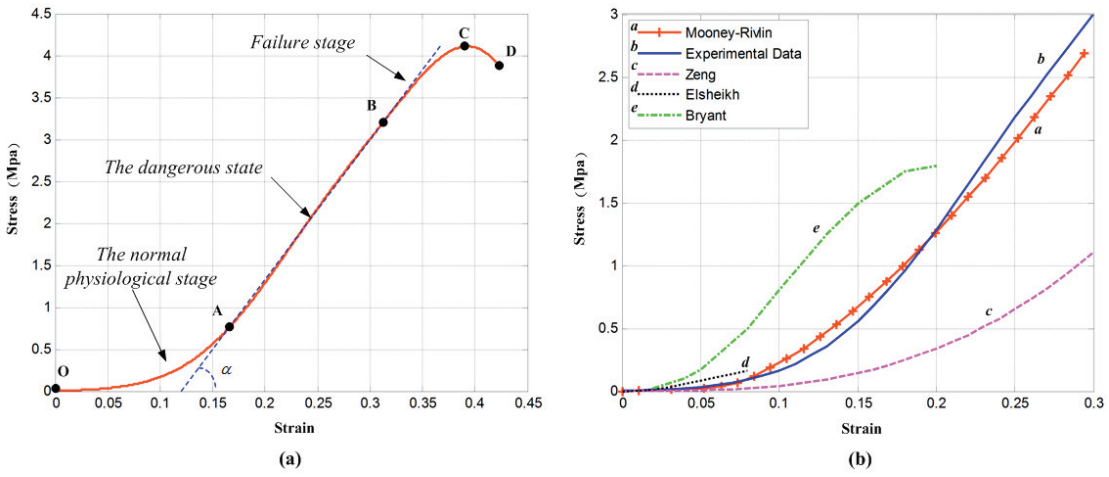

Fig. 4. The relationship curves of corneal stress-strain. (a) Fitting curve based on test results corresponding to equation (27); (b) Comparison diagram in different testing conditions. ***a*** Numerical simulation curve based on Mooney–Rivlin coefficient in ABUQUS; ***b*** The stage OB of figure (a); ***c*** Zeng et al. [30], fitting curve over ten tests; ***d*** Elsheikh et al. [9], fitting curve over thirty-four tests; ***e*** Bryant et al. [5], average value curve of nine tests

Table 2. Statistics on corneal stress–strain in uniaxial tensile tests

Test Group	Point A		Point B		Point C	
	Stress (MPa)	Strain	Stress (MPa)	Strain	Stress (MPa)	Strain
i	0.74	0.21	3.21	0.35	4.14	0.42
ii	0.68	0.15	2.51	0.29	3.92	0.35
iii	0.78	0.13	2.76	0.23	3.67	0.31
iv	0.74	0.19	2.99	0.33	3.74	0.41
v	0.72	0.14	3.71	0.27	4.63	0.35
vi	0.70	0.18	3.51	0.39	4.39	0.48
vii	0.83	0.20	2.89	0.31	3.22	0.43
viii	0.64	0.12	3.92	0.27	4.66	0.34
ix	0.77	0.20	3.83	0.37	4.59	0.45
x	0.79	0.19	3.16	0.33	4.14	0.38
Mean	0.74	0.17	3.25	0.31	4.11	0.39
Variance	0.057	0.032	0.479	0.049	0.477	0.054

$$\sigma(\varepsilon) = 3.51\exp\left(-\left(\frac{\varepsilon - 0.41}{0.10}\right)^2\right) + 2.11\exp\left(-\left(\frac{\varepsilon - 0.28}{0.11}\right)^2\right). \quad (27)$$

As can be seen from Fig. 4(a), there are three demarcation points (i.e., A, B, and C) on the curve, and the statistical data of ten tests is shown in Table 2. Firstly, the corneal tissue is in a normal physiological stage before point A, and corneal stress is nonlinear rising with the strain. Secondly, stress-strain relation of the cornea presents an obvious linear feature in the dangerous stage (as shown in the stage AB), which means corneal tissue will not be damaged during a short period. However, the overall function of the cornea will gradually deteriorate under this state for a long term. Finally, cornea will lose activity in failure stage, i.e., the stage BD, and corneal strip has broken due to excessive load at point C. In our case, corneal hyperelastic model does not consider the mechanical properties in the failure stage. Based on test data in stage OB, the Mooney–Rivlin coefficients can be determined, i.e., C_{10} = 10.59 and C_{01} = –11.20. So, the Mooney–Rivlin hyperelastic constitutive model of the cornea may be described as

$$W = 10.59(\bar{I}_1 - 3) - 11.20(\bar{I}_2 - 3). \quad (28)$$

It shows that equation (28) is the fitting equation of high-precision for test datas. Hyperelastic property of the cornea is simulated to verify the above constitutive model and measure the effectiveness of the model in ABAQUS. Assuming cornea is homogeneous material with uniform mechanical property, and strip model of the cornea is established based on Mooney–Rivlin coefficients. Simulation data are output by post-processor. The simulation curve of corneal stress-strain, as shown in the curve ***a*** of Fig. 4(b), shows a nonlinear feature.

Similarly, stress-relaxation tests of corneal strip have been carried out to determine viscoelastic parameters of the cornea. The strips are stretched up to 1.25 times their length (i.e., 4 mm) at 120 mm/min. Maintaining this status, the related data are collected at the frequency of 10 Hz. Ten times tests would be done respectively, and statistics of initial stress and last stress are shown in Table 3. The time is set to 1000 s when the stress has been basically stable. Otherwise, biological tissue will lose its original property due to dehydration.

Table 3. Statistics on stress in stress-relaxation tests (MPa)

Test Group	Initial stress	Last stress
i	2.61	0.96
ii	2.98	1.11
iii	1.96	0.86
iv	2.36	0.77
v	1.90	0.84
vi	2.25	0.81
vii	2.10	0.69
viii	2.39	0.84
ix	2.91	1.02
x	1.87	0.89
Mean	2.33	0.88
Variance	0.40	0.12

According to corneal viscoelastic model, i.e., equation (20), the number of [M] model requires special consideration. In order to describe the mechanical behavior and calculation speed, the study finds that corneal stress-relaxation can be accurately reflected when $i = 4$, taking the model accuracy into consideration. The mathematical expression is a relatively simple viscoelastic model. Based on normalization of the data from the ten tests, corneal stress-relaxation curve is fitted by the modified Maxwell viscoelastic model of the cornea, as shown in Fig. 5(a). And the model may be described as

$$G(t) = \sum_{i=1}^{4} E_i e^{-t/\tau_i} + E_5 , \qquad (29)$$

where E_i is relaxation modulus (unit: MPa), and τ_i is relaxation time (unit: s), expressed by

$$(E_1, E_2, E_3, E_4, E_5) = (0.69,\ 0.43,\ 0.31,\ 0.40,\ 0.43)$$

and

$$(\tau_1, \tau_2, \tau_3, \tau_4) = (8.83,\ 65.33,\ 876.93,\ 2.84\times10^3) .$$

It is observed that the behavior of the cornea is composed of an immediate stiff response, a transient relaxation phase, and a final steady-state stage, under stepwise stress-relaxation compression [14]. In the final steady-state stage, the stable value reflects internal residual stress of the cornea. The viscoelastic model described by equation (29) sets the non-linear relation between stress and strain. According to the test conditions and results, its elastic part is linear when elastic strain is less than 0.25 for corneal material experiment.

Corneal viscoelastic model based on Prony coefficient is simulated in ABUQUS, and the normalized curve of stress-relaxation property is shown in the curve ***a*** of Fig. 5(b). By comparing curve ***a*** with curve ***b*** in the figure, it can be observed that the simulated results are consistent with the experimental data. Moreover, the original data reported by different authors are summarized in Fig. 4(b) and Fig. 5(b), where Bryant et al. [5] tested corneal mechanical properties in the pressure eye, Elsheikh et al. [9] and Zeng et al. [30] measured corneal material properties by uniaxial tensile test. As described in the Introduction, some differences between the sets of test results are observed because of different testing conditions or testing protocols, but the results are consistent about scope and trend.

3.2. Verification by extrusion *in vivo* cornea

Using Instron 5848 Micro Tester, extrusion experiments of in vivo porcine cornea have been done, as shown in Fig. 6. The eye should be embedded in a vessel that had been fixed in the workbench, as shown in figure (b). Extrusion velocity is 1 mm/s. Eight experiments would be done respectively to obtain accurate data, including extrusion force and displacement. Fitting the average value measured by eight experiments, the relationship between force and displacement is shown in the curve ***a*** of Fig. 7(a). As can be seen from the curve, the force is approximated nonlinear growth with the increment of extrusion displacement in general.

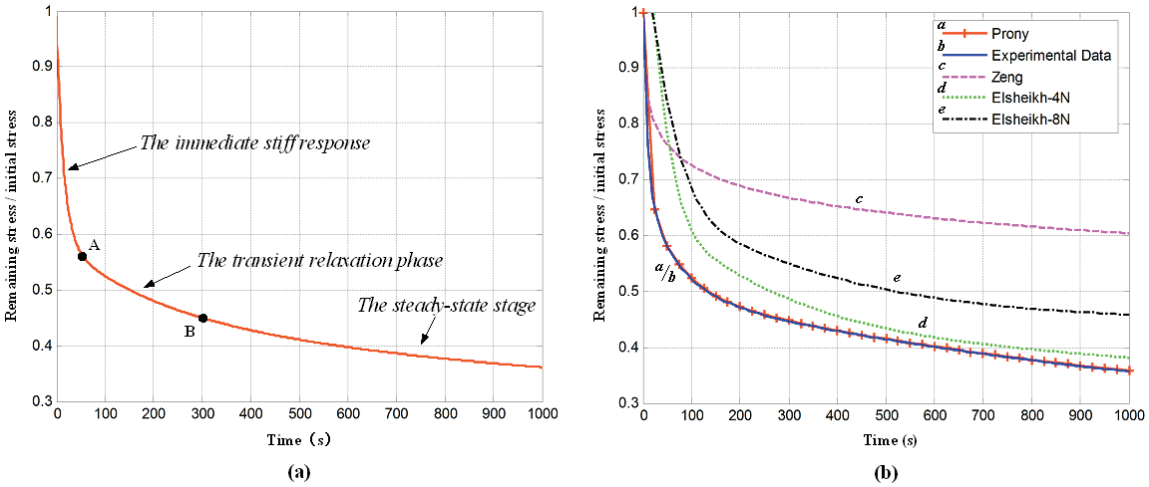

Fig. 5. Corneal stress-relaxation curves. (a) Test results corresponding to equation (29).
(b) Comparison diagram in different testing conditions. ***a*** Numerical simulation curve based on Prony coefficient in ABUQUS; ***b*** Figure (a); ***c*** Zeng et al. [30], fitting curve over ten tests; ***d*** and ***e*** Elsheikh et al. [9], tested with 4 N and 8 N max load

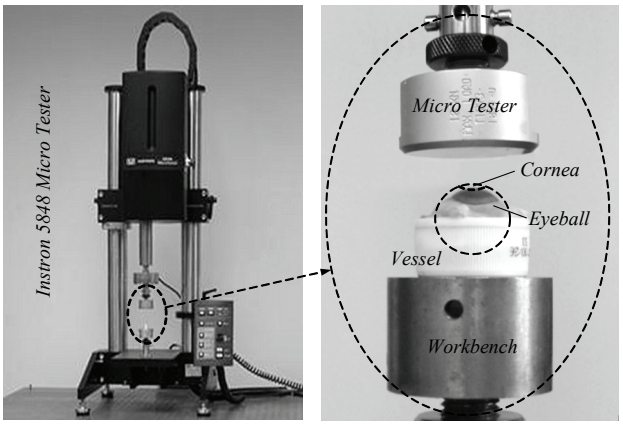

(a) (b)

Fig. 6. Corneal extrusion experiment:
(a) experimental installation,
(b) local amplification of the experiment

Then, based on corneal hyper-viscoelastic model above, the process of extrusion in vivo cornea was simulated in ABAQUS. It provides a quantitative judgment basis for corneal deformation and verifies the IOP and corneal constraints in surgery simulation.

- Modeling. According to the eyeball structure described in Fig. 1 and Table 1, eyeball model can be built in ABAQUS, where the corneal material properties are set as the same as the simulation above. Based on the actual state of the eye, cornea is constrained by sclera which is simplified as an elastomer, and material behaviors of the sclera can be described by elastic modulus $E = 3.08$ MPa and Poisson's ratio $\mu = 0.49$ [2], [3].
- Load. The lower hemisphere of the eyeball is fixed, as shown in Fig. 8(a). The briquetting presses cornea with a speed of 1 mm/s, and the extrusion time is 4 s. Besides, the value of IOP is 17.5 mm Hg (i.e., 2.33×10^{-3} MPa).
- Interaction. The lower surface of briquetting is set as master surface of interaction, and the outer surface of the eyeball is the slave surface. Interaction is edited to finite sliding, discretization method of surface to surface, frictionless tangential behavior, and pressure-overclosure normal behavior of hard-contact.

The extrusion results of experiment and simulation are shown in Fig. 7(a). Obviously, there are two relatively distinct inflection points A and B in the force-displacement curves. Analyzing corneal structure and the extrusion process, stage OA indicates the deformation of central pupillary zone, and the zone is flattened at point A corresponding to Fig. 8(a). Stage OB manifests the deformation of whole cornea, and the cornea is flattened at point B corresponding to Fig. 8(b). During extrusion process, the force is growing exponentially at the beginning, and the rising trend reaches the minimum at point B due to the impact of connecting structure between cornea and sclera. The force will rapidly increase again with displacement after point B, and sclera and other structures of the eye are extruded in the stage. By comparing the two curves, the change of the simulation curve is more noticeable, since it is obtained in the ideal conditions.

The displacements for the hyperelasticity do not depend on time. Certainly, different extrusion velocities are set to determine the difference with the viscoelasticity as the velocity of loading, and the results show that the difference is barely noticeable. In order to explain the necessity of IOP, extrusion simulation results under different IOP are shown in Fig. 7(b). The simulation can not be completed if IOP is set too small. For example, the simulation was interrupted at 2.35 or 2.65 mm when $P = 0$ or 1.75 mmHg. Similarly, if IOP is set too large, e.g., $P = 175$ mmHg, it is inconsistent with the actual situation that the force will change too much with the displacement.

In the extrusion simulation, parts of stress and strain nephograms are described in Fig. 8. Corneal central pupillary zone flattened at the displacement is 1.1 mm, as shown in figure (a); the whole cornea is flattened, as depicted in figure (b) and (d). In figure (c), significant elastic deformation occurred at unconstrained sclera in addition to extrusion of the cornea. Of course, there are many factors affecting eyeball deformation, e.g., local deformation, unequal force, etc. So, the simulation can only simulate corneal deformation in ideal conditions due to limitations of parameter settings.

4. Discussion

Currently, many scholars have done a lot of work and achieved some results in corneal biomechanics, but it still encounters with various problems in clinical application. This paper discusses a biomechanical model that relates to the significant characteristics of corneal material: hyperelastic and viscoelastic. The ability of the model to reproduce the behavior of human cornea opens a promising perspective for numerical simulation of corneal microsurgery.

The constitutive models of hyperelastic material include neo-Hookean model, polynomial form model, Yeoh model, and Mooney–Rivlin model, etc. [17].

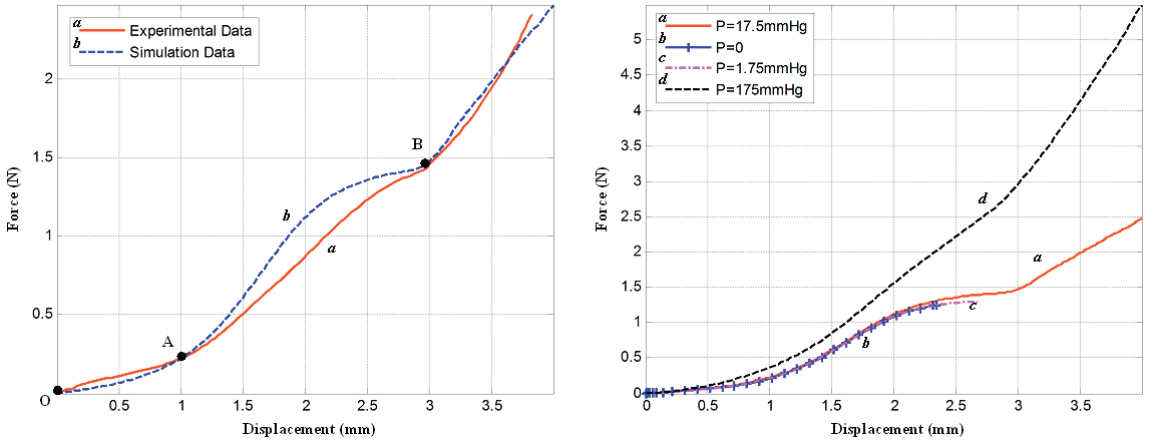

(a) (b)

Fig. 7. The relationship curves between extrusion force and displacement.
(a) Comparison diagram between experiment and simulation.
a The fitting results for average values of extrusion experiment; ***b*** Simulation curve under normal IOP.
(b) Comparison diagram in different IOP, where ***a***, ***b***, ***c***, and ***d*** represent the curve when IOP is 17.5 mmHg, 0 mmHg, 1.75 mmHg, and 175 mmHg, respectively

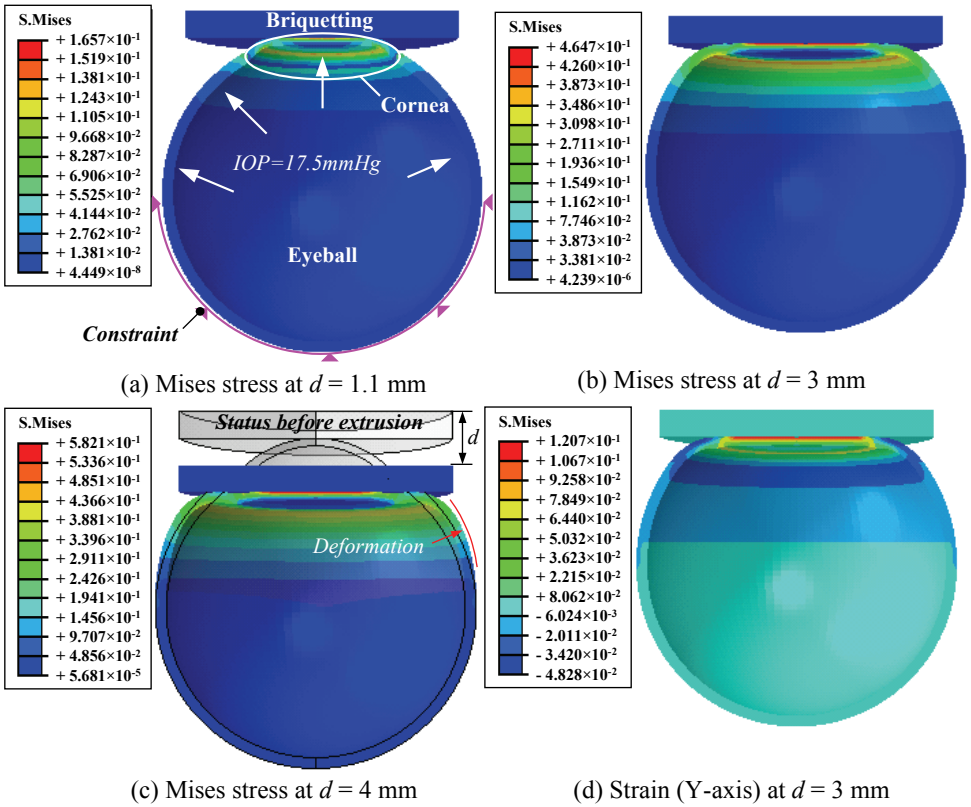

(a) Mises stress at $d = 1.1$ mm (b) Mises stress at $d = 3$ mm

(c) Mises stress at $d = 4$ mm (d) Strain (Y-axis) at $d = 3$ mm

Fig. 8. Stress–strain nephograms of the eye in extrusion simulation, where (a), (b), and (c) represent Mises stress nephograms when extrusion displacement is 1 mm, 3 mm, and 4 mm, respectively. And (d) is elastic strain nephogram on *y*-axis direction when the displacement is 3 mm. In figure (c), the gray wire frame describes the state before being extruded, where *d* indicates the displacement of extrusion

The Mooney–Rivlin model is most widely used in finite element analysis because it is simple and practical, and it can describe the mechanical properties of the homogeneous hyperelastic materials under large deformation. Hyperelastic model of the cornea has been built based on Mooney–Rivlin theory, which can be simplified as a linear equation with two unknowns after a series of mechanical derivation. In the vis-

coelastic mechanics, a modified Maxwell model is constructed where an elastic element is connected in parallel with the generalized Maxwell model. Comparing with the existing viscoelastic model such as Burgus model, modified Burgus model, and generalized Maxwell model [2], [13], the modified Maxwell model of the cornea is simple and intuitive, and it can accurately describe viscoelastic of corneal material. If the action time of the external load is longer enough, the internal stress of the material will gradually close to a fixed value [14], which can be shown by paralleled elastic element [E] in the model.

There are two means to describe the biomechanical properties of the cornea: swelling test of in vitro cornea and tensile test of corneal strip [5], [16]. The swelling test is close to physiological state of the cornea, but it can only obtain one-dimensional data of the material. Although affected by the initial state, the tensile test can reflect corneal anisotropy. In order to get accurate data under our testing condition that is consistent with the later extrusion experimentation, the parameters of corneal hyper-viscoelastic model have been obtained by uniaxial tensile test and stress relaxation test. They describe the biomechanical properties that are broadly in line with the results of previous publication, even though there are some differences in the accurate results due to different testing conditions [5], [9], [29], [30]. Based on the hyper-viscoelastic model, the stress-strain relationship and stress-relaxation characteristic are presented in the simulation of corneal material. Taken together, simulations and tests show consistent results to validate the validity and applicability of the hyper-viscoelastic model in ABAQUS.

In corneal microsurgery, cornea is one part of the eye rather than as strip isolated. So, an in vivo model of the cornea is built, which can be used to simulate diagnosis and treatment of corneal disease, and it is validated by extrusion experiment and simulation. In the eyeball, there is close association between cornea and sclera, and they together constitute the outer wall of the eye. So the cornea is constrained by the sclera that is simplified as an elastomer, and the results show that it is an effective way to deal with constraint problem of the cornea.

Cornea will be deformed during surgery, wherein the deformation in vertical direction is not only completely caused by the cornea, but also includes deformation of the whole eyeball. This property, which reflects eyeball deformation under loads, is called overall stiffness of the eyeball. Previous research data show that the stiffness in various parts of the eyeball makes a little difference, and the relationship between extrusion force and displacement can serve as a useful reference for overall stiffness of eyeball [1], [23]. In general, the force–displacement curve obtained by the simulation is consistent with the experimental result, and some differences can be ignored as the reality organisms always have some factors that can not be simulated, such as local deformation and unequal force.

In this paper, the porcine cornea is taken as the test subject to determine the hyper-viscoelastic model of the cornea. The human cornea has a siginificantly different anatomical construction, and in mechanics, it is significantly stiffer than the porcine cornea so that the human cornea can sustain the stress for longer under long-term loading. The porcine cornea is not an acceptable substitute for a human cornea [9]. But this paper discusses hyper-viscoelastic property of the cornea to construct a biomechanical model, which does not involve the physiological state, and in this respect there are some similarities between human and pig. The proposed method has the certain adaptability in biomechanical research of human cornea.

This hyper-viscoelastic model is relatively simple and suitable for digital modeling of corneal material. We are evaluating the possibility to perform the simulation of corneal surgery based on the results of this study. With further biomechanical research we will explore ways to implement real-time simulation of keratoplasty combining robotics and finite element methods.

Acknowledgement

The authors wish to thank the National Natural Science Foundation of China (Grant No. 50675008 and Grant No. 51175013) that supported this work.

References

[1] ANDERSON K., EL-SHEIKH A., NEWSON T., *Application of structural analysis to the mechanical behaviour of the cornea*, J. R. Soc. Interface, 2004, 1(1), 3–15.

[2] ASEJCZYK-WIDLICKA M., SRODKA W., SCHACHAR R.A., PIERSCIONEK B.K., *Material properties of the cornea and sclera: A modelling approach to test experimental analysis*, J. Biomech., 2011, 44(3), 543–546.

[3] BATTAGLIOLI J.L., KAMM R.D., *Measurements of the compressive properties of scleral tissue*, Invest. Ophth. Vis. Sci., 1984, 25(1), 59–65.

[4] BERKLEY J., TURKIYYAH G., BERG D., GANTER M., WEGHORST S., *Real-time finite element modeling for surgery simulation: An application to virtual suturing*, IEEE T Vis. Comput. Gr., 2004, 10(3), 314–325.

[5] BRYANT M.R., MCDONNELL P.J., *Constitutive laws for biomechanical modeling of refractive surgery*, J. Biomech. Eng.-T ASME, 1996, 118(4), 473–481.

[6] CHRISTENSEN R.M., *Theory of Viscoelasticity*, Academic Press, New York, 1982.
[7] DOGHRI I., *Nonlinear continuum mechanics*, Springer, Berlin–Heidelberg, 2000.
[8] EHLERS N., HJORTDAL J., *Corneal thickness: measurement and implications*, Exp. Eye Res., 2004, 78(3), 543–548.
[9] ELSHEIKH A., ALHASSO D., RAMA P., *Biomechanical properties of human and porcine corneas*, Exp. Eye Res., 2008, 86(5), 783–790.
[10] ETHIER C.R., JOHNSON M., RUBERTI J., *Ocular biomechanics and biotransport*, Annu. Rev. Biomed. Eng., 2004, 6, 249–273.
[11] FRATZL P., MISOF K., ZIZAK I., *Fibrillar structure and mechanical properties of collagen*, J. Struct. Biol., 1998, 122(1), 119–122.
[12] HAMEED-SAYED A.A., SOLOUMA N.H., EL-BERRY A.A., KADAH Y.M., *Finite element models for computer simulation of intrastromal photorefractive keratectomy*, J. Mech. Med. Biol., 2011, 11(05), 1255–1270.
[13] HATAMI-MARBINI H., *Viscoelastic shear properties of the corneal stroma*, J. Biomech., 2014, 47(3), 723–728.
[14] HATAMI-MARBINI H., ETEBU E., *An experimental and theoretical analysis of unconfined compression of corneal stroma*, J. Biomech., 2013, 46(10), 1752–1758.
[15] HENDRIKS F.M., BROKKEN D., OOMENS C.W., BADER D.L., BAAIJENS F.P., *The relative contributions of different skin layers to the mechanical behavior of human skin in vivo using suction experiments*, Med. Eng. Phys., 2006, 28(3), 259–266.
[16] HJORTDAL J.O., *Regional elastic performance of the human cornea*, J. Biomech., 1996, 29(7), 931–942.
[17] HOLZAPFEL G.A., *Nonlinear solid mechanics*, Chichester, Wiley, 2000.
[18] KAMPMEIER J., RADT B., BIRNGRUBER R., BRINKMANN R., *Thermal and biomechanical parameters of porcine cornea*, Cornea, 2000, 19(3), 355–363.
[19] KARALIS T.K., *A model for corneal swelling*, J. Mech. Med. Biol., 2008, 8(04), 473–489.
[20] KUNTER F.C., SEKER S.S., *Web-spline prediction of ocular supface temperature using bioheat equation with external source exposure*, J. Mech. Med. Biol., 2013, 14(1), 1450009.
[21] LI L., TIGHE B., *The anisotropic material constitutive models for the human cornea*, J. Struct. Biol., 2006, 153(3), 223–230.
[22] OGDEN R.W., *Non-linear elastic deformations*, Courier Dover Publications, 1997.
[23] PANDOLFI A., MANGANIELLO F., *A model for the human cornea: constitutive formulation and numerical analysis*, Biomech. Model Mechan., 2006, 5(4), 237–246.
[24] PINSKY P., VAN-DER-HEIDE D., CHERNYAK D., *Computational modeling of mechanical anisotropy in the cornea and sclera*, J. Cataract. Refract. Surg., 2005, 31(1), 136–145.
[25] SCHAPERY R.A., *Nonlinear viscoelastic solids*, Int. J. Solids Struct., 2000, 37(1), 359–366.
[26] STUDER H., LARREA X., RIEDWYL H., BUCHLER P., *Biomechanical model of human cornea based on stromal microstructure*, J. Biomech., 2010, 43(5), 836–842.
[27] THOMASY S.M., RAGHUNATHAN V.K., WINKLERB M., REILLY C.M. et al., *Elastic modulus and collagen organization of the rabbit cornea: Epithelium to endothelium*, Acta Biomater., 2014, 10(2), 785–791.
[28] WILDNAUER R.H., BOTHWELL J.W., DOUGLASS A.B., *Stratum corneum biomechanical properties I. Influence of relative humidity on normal and extracted human stratum corneum*, J. Invest. Dermatol., 1971, 56(1), 72–78.
[29] WOO S.L., KOBAYASHI A.S., SCHLEGEL W.A., LAWRENCE C., *Nonlinear material properties of intact cornea and sclera*, Eep. Eye Res., 1972, 14(1), 29–39.
[30] ZENG Y., YANG J., HUANG K., LEE Z., LEE X., *A comparison of biomechanical properties between human and porcine cornea*, J. Biomech., 2001, 34(4), 533–537.